Science of the Total Environment 609 (2017) 92–101

Contents lists available at ScienceDirect

Science of the Total Environment

journal homepage: www.elsevier.com/locate/scitotenv

River sequesters atmospheric carbon and limits the CO_2 degassing in karst area, southwest China

Tao Zhang [a,b], Jianhong Li [a], Junbing Pu [a,*], Jonathan B. Martin [c], Mitra B. Khadka [c], Feihong Wu [a,b], Li Li [a,b], Feng Jiang [d], Siyu Huang [a], Daoxian Yuan [a,b]

[a] Key Laboratory of Karst Dynamics, MLR & Guangxi, Institute of Karst Geology, Chinese Academy of Geological Sciences, Guilin 541004, China
[b] Chongqing Key Laboratory of Karst Environment, School of Geography Sciences, Southwest University, Chongqing 400715, China
[c] Department of Geological Sciences, University of Florida, Gainesville, FL 32611, USA
[d] College of Environmental Science and Engineering, Guilin University of Technology, Guilin 541004, China

HIGHLIGHTS

- Significant diel variations occur in CO_2 uptake and evasion in a karst river.
- A river can be both sink and source of atmospheric CO_2 at different timescales.
- Biological processes of sub-aquatic community control river CO_2 uptake and evasion.
- Karst rivers degas less CO_2 to the atmosphere than non-karst rivers in the world

GRAPHICAL ABSTRACT

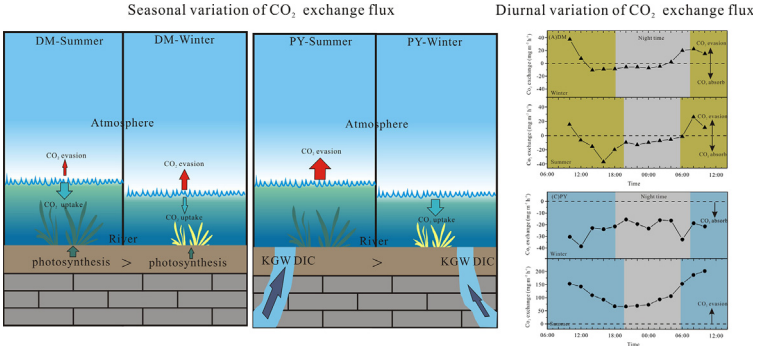

ARTICLE INFO

Article history:
Received 20 May 2017
Received in revised form 13 July 2017
Accepted 16 July 2017
Available online xxxx

Editor: D. Barcelo

Keywords:
CO_2 uptake
Water-air interface
Diel cycle
Karst river
Southwest China

ABSTRACT

CO_2 fluxes across water-air interfaces of river systems play important roles in regulating the regional and global carbon cycle. However, great uncertainty remains as to the contribution of these inland water bodies to the global carbon budget. Part of the uncertainty stems from limited understanding of the CO_2 fluxes at diurnal and seasonal frequencies caused by aquatic metabolism. Here, we measured surface water characteristics (temperature, pH, and DO, DIC, Ca^{2+} concentrations) and CO_2 fluxes across the air-water interface at two transects of Guijiang River, southwest China to assess the seasonal and diurnal dynamics of fluvial carbon cycling and its potential role in regional and global carbon budgets. The two transects had differing bedrock; DM transect is underlain by carbonate and detrital rock and PY is underlain by pure carbonate. Our results show that the river water both degasses CO_2 to and absorbs CO_2 from the atmosphere in both summer and winter, but the degassing and absorption varied between the two transects. Further, CO_2 fluxes evolve through diurnal cycles. At DM, the river evaded CO_2 from early morning through noon and absorbed CO_2 from afternoon through early morning. At PY in summer, the CO_2 evasion decreased during the daytime and increased at night while in winter at night, CO_2 uptake increased in the morning and decreased in the afternoon but remained relatively stable at night. Although the river is a net source of carbon to the atmosphere (~15 mM m^{-2} day^{-1}), the evasion rate is the smallest of all reported world's inland water bodies reflecting sequestration of atmospheric carbon through the carbonate dissolution and high primary productivity. These results emphasize the need of seasonal and

* Corresponding author at: Institute of Karst Geology, Chinese Academy of Geological Sciences, NO.50, Qixing Ave, Qixing District, Guilin 541004, China.
E-mail address: junbingpu@karst.ac.cn (J. Pu).

http://dx.doi.org/10.1016/j.scitotenv.2017.07.143

diurnal monitoring of CO_2 fluxes across water-air interface, particularly in highly productive rivers, to reduce uncertainty in current estimates of global riverine CO_2 emission.

1. Introduction

Rivers play an important role in the global carbon cycle by linking terrestrial and marine carbon reservoirs. An important role of river systems in the global carbon cycle involves biogeochemical transformations and delivery of terrestrially derived organic and inorganic carbon to the ocean, which are estimated to be 0.4–0.8 and 0.4 Pg C yr^{-1}, respectively (Degens et al., 1991). In addition to delivery of C to the ocean, river systems also exchange CO_2 with the atmosphere across the water–air interface. Many studies have shown that rivers are usually supersaturated with respect to CO_2, which results in evasion of much CO_2 to the atmosphere (Yang et al., 1996; Richey et al., 2002; Jones et al., 2003; Yao et al., 2007; Wang et al., 2007), leading to the suggestion that CO_2 emissions from rivers could be an important component of the global carbon budget.

The first regional estimate of riverine CO_2 degassing was conducted in the Amazon Basin, and was estimated to be 0.47 Pg C yr^{-1} (Richey et al., 2002). Butman and Raymond (2011) estimated that the contiguous United States streams and rivers degassed ~0.1 Pg C yr^{-1}, which they extrapolated to be 0.5 Pg C yr^{-1} for temperate rivers between latitudes 25° and 50° north. Recently, Borges et al. (2015) integrated CO_2 degassing for all sub-Saharan African rivers, which ranged from 0.27 to 0.37 Pg C yr^{-1}. Although these studies constrain regional atmospheric CO_2 evasion from inland waters, global estimates are limited and poorly constrained, with a range from 0.23 to 2.1 Pg C yr^{-1} (Cole et al., 2007; Tranvik et al., 2009; Aufdenkampe et al., 2011; Regnier et al., 2013; Raymond et al., 2013). These estimates range over nearly an order of magnitude as a result of large uncertainty in the data. Regardless of the poor constrains on the global estimates, CO_2 degassing appears to be about twice as large as lateral export of carbon to the coastal ocean from the global river network (Bauer et al., 2013; Regnier et al., 2013). Even though these fluxes appear to be small fractions of the global C cycle, they are significant compared to the net oceanic uptake of anthropogenic CO_2 of 2 Pg C yr^{-1} (Sarmiento and Sundquist, 1992). Thus, it is important to assess CO_2 fluxes across water-air interface in rivers for better constraints on the regional and global carbon budget and cycle.

Some of the uncertainty of riverine CO_2 fluxes may result from variations in catchment lithology and through time, neither of which has been extensively evaluated. CO_2 degassing decreases as rivers drain from siliciclastic to carbonate terrains due to rapid kinetics of carbonate minerals dissolution and photosynthetic uptake of DIC in the clear-water karst river systems (Khadka et al., 2014; Martin, 2017). In addition, rivers' diurnal dynamic nature of biogeochemical cycles driven by daily differences in temperature and solar radiation results in changes of pH, DIC, DO and CO_2 concentrations at diurnal frequency, particularly in karst rivers due to their clear, carbon-enriched water (Liu et al., 2006, 2008; de Montety et al., 2011; Nimick et al., 2011; Pu et al., 2017). Diurnal cycles of river water chemistry should also cause significant diurnal variations in CO_2 fluxes across the water-air interface (Pu et al., 2017). Hence, diurnal variations as well as seasonal variations in CO_2 evasion needs to be evaluated to improve estimates of regional and global carbon fluxes in river systems. However, time series measurements of diurnal and seasonal changes in CO_2 evasion are rare.

To improve the constraints on riverine CO_2 fluxes, we measured the diurnal and seasonal concentrations of river water chemistry and CO_2 fluxes across water-air interface in a subtropical karst river (Guijiang River; GJR) located in southwest China. We use these data to assess the seasonal and diurnal dynamics of carbon cycles and their potential role in regional and global carbon budgets. We estimated magnitude and direction of CO_2 fluxes at high temporal resolution using time series physico-chemistry data, as well as employing the floating chamber (FC) and the thin boundary layer (TBL) methods. These observations indicate seasonal and diurnal CO_2 flux estimates must be considered in regional and global estimates of riverine CO_2 fluxes to minimize uncertainty of the estimates.

2. Materials and methods

2.1. Study area

The Guijiang River, a tributary of the Pearl River, originates in Maoershan Mountain at an elevation of 2142 m (Fig. 1). The river is 438 km long and drains an area of 18,790 km^2. Average river gradient, runoff depth and annual runoff are 0.43%, 1033 mm and 1.44 $\times 10^{10}$ m^3/yr, respectively. The regional climate is dominated by the East Asian Monsoon, characterized by a cold–dry winter from late November through March and a hot–rainy summer from April through October. Average local annual precipitation is 1666 mm, with 72.1% of the rainfall occurring in the wet season. Annual average temperature is about 20 °C in the GJR catchment. Based on the type and age of catchment rocks, the river can be divided into three reaches. The upper reach, upstream to the Rongjiang Town, is primarily composed of Silurian granites, Ordovician–Cambrian shales, and mud rocks intercalated with carbonate rocks. The middle reach, from the confluence with the Lingqu River to Pingle County, also called "the Lijiang River", is almost entirely underlain with Devonian carbonate rocks. The lower reach flows across the Cambrian terrain composed of largely carbonate rocks intercalated with shales.

Two monitoring sites were selected for high-resolution diel monitoring and sampling (Fig. 1). The upstream site, DM (25°20′59″N, 110°19′21″E) is located at the upstream edge of the middle reach, and is 6–9 m deep, 120 m wide and underlain by carbonate and siliciclastic rock. The downstream site, PY (24°40′37″N, 110°35′59″E) is located at the downstream edge of the middle reach, and is approximately 100 km downstream from DM, 0.5–2 m deep and 220 m wide and is underlain by pure carbonate rocks.

2.2. Hydrochemical parameters

Temperature, pH, dissolved oxygen (DO), turbidity (Tb) and specific conductivity (SpC) were measured in situ at 15-min time interval at both sites DM and PY using multi-parameters meter (YSI Pro Dss, Yellows Springs, Ohio, USA) between August 24 to August 28, 2016 and Dec 15 to Dec 18, 2016. Prior to each deployment, the instrument was calibrated according to manufacturer's specifications using pH buffers 4.00, 7.00 and 10.00, and a 1413 μS cm^{-1} solution for SpC. The DO probe was calibrated with water saturated moist air. Resolutions for temperature, pH, DO, Tb and specific conductivity (SpC) are 0.1 °C, 0.01 pH unit, 0.01 mg/L, 0.03 NTU and 1 μS cm^{-1}, respectively.

2.3. Discrete sample collection and analysis

Discrete river waters were sampled every 2 h at both sites by using syringes. Each sample was immediately filtered through 0.45 μm filter membranes and was collected in pre-rinsed high density polyethylene (HDPE) bottles (500 ml) for major ion analyses. Samples for cations were acidified to pH < 2 with HNO_3. All samples were stored in an ice box until delivered to the laboratory, where they were kept chilled in a refrigerator at 4 °C until analysis. Alkalinity was determined using

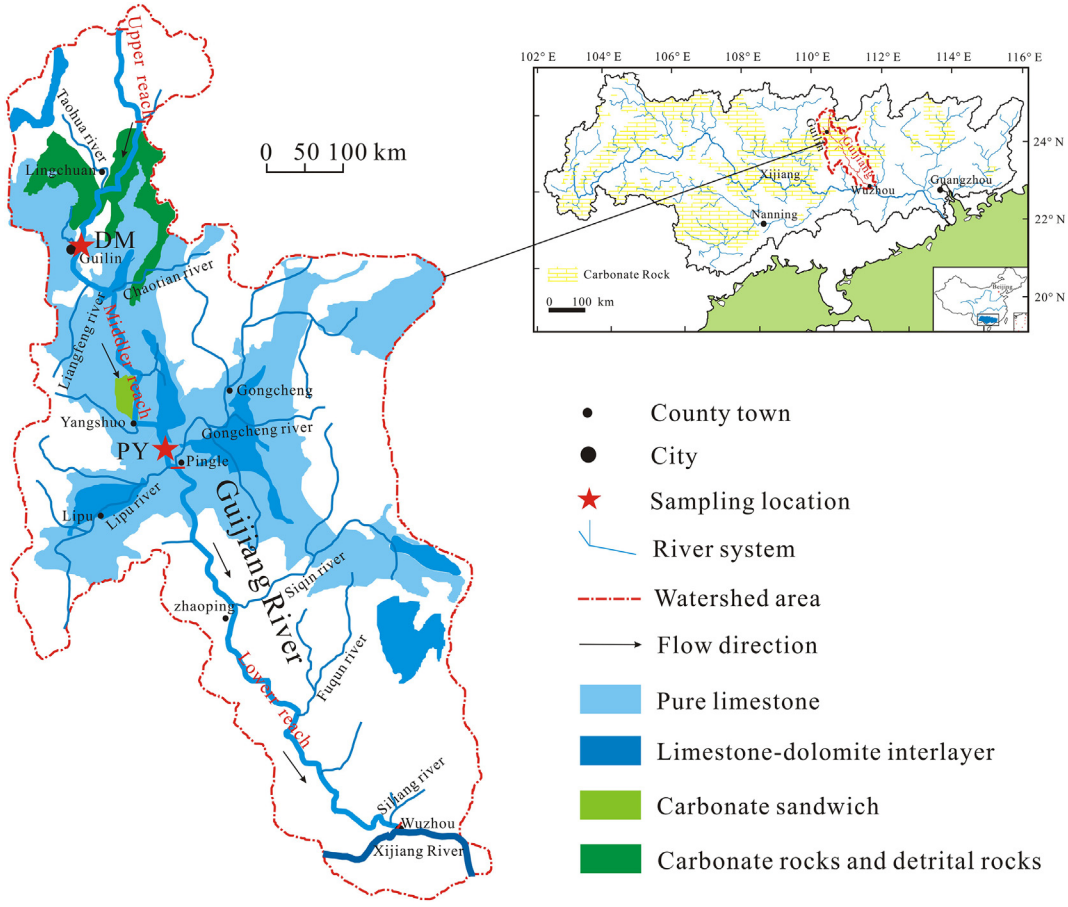

Fig. 1. Map of the Guijiang River catchment and sampling locations (Modified from Sun et al., 2015).

HCl titration with a Titrette Digital Titrator (Brand Trading *Co*., Ltd., Wertheim, Germany). The titrant was 0.1 mmol L^{-1} HCl and the titration endpoint was pH = 4.5.

Major anions (Cl^-, SO_4^{2-}, NO_3^-) were measured by an automated Dionex ICS-900 ion chromatograph based on APHA 2012 method (Rice et al., 2012). Major cations (Ca^{2+}, Mg^{2+}, K^+ and Na^+) were analyzed by ICP–OES (IRIS Intrepid II XSP, Thermo Fisher Scientific, USA) using a procedure based on EPA method 200.7. Estimated analytical errors were within ±5%. All laboratory analyses were carried out in the Environmental and Geochemical Analysis Laboratory at the Institute of Karst Geology, Chinese Academy of Geological Science.

The hydrochemical data sets, including pH, water temperature and concentrations of K^+, Na^+, Ca^{2+}, Mg^{2+}, Cl^-, SO_4^{2-} and HCO_3^- were processed with the program WATSPEC (Wigley, 1977) to calculate partial pressure of CO_2 (pCO_2) and saturation index of calcite (SIc) in river water. pCO_2 is assumed to be in equilibrium with the sampled waters by the equation:

$$pCO_2 = \frac{(HCO_3^-)(H^+)}{K_1 K_h} \quad (1)$$

where species in parentheses are activities of corresponding species in mol L^{-1}, and $K_1$and K_h are the temperature-dependent first dissociation constant for H_2CO_3 and Henry's Law constant, respectively. SIc was calculated using equation:

$$SIc = \mathrm{Log}\left(\frac{IAP}{K}\right) \quad (2)$$

where IAP is the ion activity product and K is the temperature–dependent equilibrium constant of calcite or dolomite dissolution. If SIc = 0, water is in thermodynamic equilibrium; if SIc < 0, water is under-saturated; and if SIc > 0, water is supersaturated with respect to calcite or dolomite.

2.4. CO_2 fluxes across the water-air interface

2.4.1. Thin boundary layer method (TBL)

CO_2 fluxes across the water-air interface were calculated using the following equation based on the Fick's law (UNESCO/IHAGHG, 2010):

$$Flux = K(c_{water} - c_{air}) \quad (3)$$

where *Flux* is the CO_2 flux (mg m^{-2} h^{-1}) across water and atmosphere, *K* is the gas transfer velocity (cm h^{-1}), $c_{water} - c_{air}$ is the CO_2 concentration difference between the water and air. The atmospheric CO_2 concentration was measured by EGM-5 (PP Systems, USA) in situ. We calculated K using the temperature-dependent Schmidt number (Sc_T) for fresh water (Raymond et al., 2012):

$$K = K_{600} \times (Sc_T/600)^{-0.5} \quad (4)$$

with

$$Sc_T = 1911.1 - 118.11T + 3.4527T^2 - 0.04132T^3 \quad (5)$$

where T is the in situ water temperature (°C), and K_{600} is the *K* for CO_2 at 20 °C in freshwater. *K* values depend on river size (Alin et al., 2011) and

can be 60% greater in rivers with channel <100 m wide than in rivers with channel >100 m wide. Different equations are available for large and small rivers. Because the GJR width is usually >100 m throughout the year, and at both of our transects, we estimated K_{600} using the large rivers formula (Alin et al., 2011):

$$K_{600} = 4.46 + 7.11 \times {}^{-}u_{10} \quad (6)$$

where ${}^{-}u_{10}$ is wind speed 10 m above rivers, derived by:

$${}^{-}u_z = \left(\frac{u_*}{\kappa}\right) \ln\left(\frac{z}{z_0}\right) \quad (7)$$

where ${}^{-}u_z$ is mean wind speed (m s^{-1}) at the height z, u_* is friction velocity (m s^{-1}), κ is von Karman's constant (≅0.40), and z_0 is roughness length (10^{-5} m, an intermediate value for water surfaces). Wind speed was measured for 3–5 min at the time of flux measurements by handheld anemometer (KANOMAX6036, Japan, INC.), and air temperature was measured by temperature and humidity recorder (SSN-71USB, Yuan Heng Tong Technology Co. Ltd., China).

2.4.2. Floating chamber method (FC)

The floating chamber is an inexpensive and convenient method to measure direct diffusive fluxes at the surface of aquatic ecosystems. We used EGM-5 (PP Systems, USA) in conjunction to measure CO_2 concentration with a floating chamber designed independently for on-line monitoring. The floating chamber was a stainless steel cylinder with a diameter of 30 cm and a height of 40 cm; the volume of air trapped inside the chamber was 28.3 L. Interior walls of the chamber were laminated with a heat insulating material to prevent overheating due to direct sunlight, and a small fan was equipped inside the chamber to homogenize the gas. A vent on the top of the chamber equilibrated pressure inside the chamber with the atmospheric pressure prior to each measurement (Liu et al., 2014). The chamber was connected to the EGM-5 with tygon tubing in a closed loop and air was circulated through using EGM-5′s internal pump. The air coming from the chamber was passed through a desiccant to prevent water condensation in the tubing. The initial increase in pCO_2 in the chamber was plotted against time and the slope of the increase found by linear regression analysis was used to estimate the flux of CO_2 across the air-water interface by:

$$\text{Flux} = \frac{\text{Slope} \times F_1 \times F_2 \times V}{S} \quad (8)$$

with

$$F_1 = \frac{F_3 \times F_4 \times \text{AtmP}}{R \times (273.13 + T)} \quad (9)$$

where Flux is CO_2 flux (mg m^{-2} h^{-1}), Slope is the slope in the time-concentration plot (10^{-6} min^{-1}), F_1 is a conversion factor from ppm to mg m^{-3} for standard temperature and pressure (mg m^{-3}), F_2 is a conversion factor of minutes into hours (60), V is chamber volume (m^3), S is chamber surface area (m^2), F_3 is the measured CO_2 volume concentration (10^{-6}), F_4 is molecular weight of CO_2 (44 g mol^{-1}), AtmP is the measured atmospheric pressure (KPa), R is gas constant (≅8.314 J K^{-1} mol^{-1}), T is the measured air temperature (°C).

2.5. Statistical analyses

For each water sample time, CO_2 evasion was calculated by the TBL and FC methods, respectively. Relationships between CO_2 evasion and environmental parameters and hydrogeochemical characteristics, and the stoichiometric ratios of pH, pCO_2, DO, water temperature, ΔTb (ΔTb = Tb in summer − Tb in winter) and ΔpCO_2 (ΔpCO_2 = pCO_2 in summer − pCO_2 in winter), ΔFlux (ΔFlux = CO_2 exchange in summer − CO_2 exchange in winter), ΔDIC (ΔDIC = DIC in summer − DIC in winter), and ΔpH (ΔpH = pH in summer − pH in winter) were tested with linear and nonlinear regression analyses. The coefficients of variation (CV) are <10% for pH, T, and DO, except for DO in summer at DM (12.77%) and are >15% for pCO_2 and CO_2 flux, except for TBL estimate of CO_2 flux in winter at PY (16.66%). The statistical processes were conducted using software SPSS 19.0.

3. Results & discussion

3.1. Diel variation in river water chemistry

Hydrochemical changes of the two transects in the Guijiang River are shown in Fig. 2. There were minor diurnal changes in water temperature as shown by coefficients of variation (CV) that are <3% in both summer and winter at DM and PY transects. At DM, there were major diurnal changes in all parameters including pH, DO, SpC, DIC, SIc and pCO_2 (Fig. 2). All measured variables at PY showed smaller diel variation than those at DM over the sampling periods. However DIC, SIc and pCO_2 also showed obvious diel variation at PY (Fig. 2).

Hydrochemical parameters at DM in summer showed regular changes at diurnal frequencies, of which the temperature, pH, DO and SIc in the water increased during the daytime with the highest values occurring at late afternoon (18:00–20:00) and started to decrease at night with the lowest values occurring in the morning (10:00). SpC, DIC and pCO_2 of river water decreased in the daytime with the lowest values at late afternoon (18:00–22:00) and started to increase from night with the highest values occurring in the morning (10:00) (Fig. 2). In winter at DM and in summer at PY, except for SpC, these pronounced hydrochemical parameters showed similar variation pattern with different amplitudes. Hydrochemical parameters at PY in winter showed different variation pattern at diurnal frequencies. Temperature, pH, DO and SIc in the water increased in the morning with the highest values at noon and decreased in the afternoon with the lowest values at night (22:00), then increased at night, and are inversely related to DIC and pCO_2.

3.2. Comparison of TBL vs FC methods

The TBL method calculates gas flux using semi-empirical equations and consequently, mechanisms that drive the process remain poorly understood resulting in high uncertainty. Uncertainty is compounded from variable nature of correlated factors, such as wind, waves, surfactants, thermal convection or stratification, wave breaking, and upwelling (UNESCO/IHAGHG, 2010). Due to the high uncertainty of the TBL method, the floating chamber coupled with an automated instrument has recently become a commonly used technique for direct measurement of gas fluxes across the water-air interfaces (UNESCO/IHAGHG, 2010; Zhao et al., 2015).

Due to logistic constraints, we were unable to compare of the two methods simultaneously in the field and thus our comparisons rely on average flux measured in the same area during the same time period (e.g. Lambert and Fréchette, 2005). At the PY transect, the average CO_2 exchange derived from the FC method was greater than the TBL method by a factor of 2.3 in the summer and by a factor of 1.3 in the winter. However, at the DM transect the average CO_2 exchange estimated from the FC method was lower than the TBL method, by 1.9 times in the summer and 2.0 times in the winter. The TBL method overestimates the wind effect in deep water areas while it underestimates the emission when winds are light in shallow water areas (Duchemin et al., 1999). The TBL method may thus have overestimated the CO_2 fluxes from the deeper water at DM than the PY transect. Winds were light (0.01 to 3.99 m s^{-1}) at both transects and are unlikely to contribute to the differences. Regardless of the uncertainty in the two methods, the CO_2 fluxes derived from TBL and FC methods have positive correlations ($P < 0.05$) at all sampling times and places (Fig. 3), reflecting

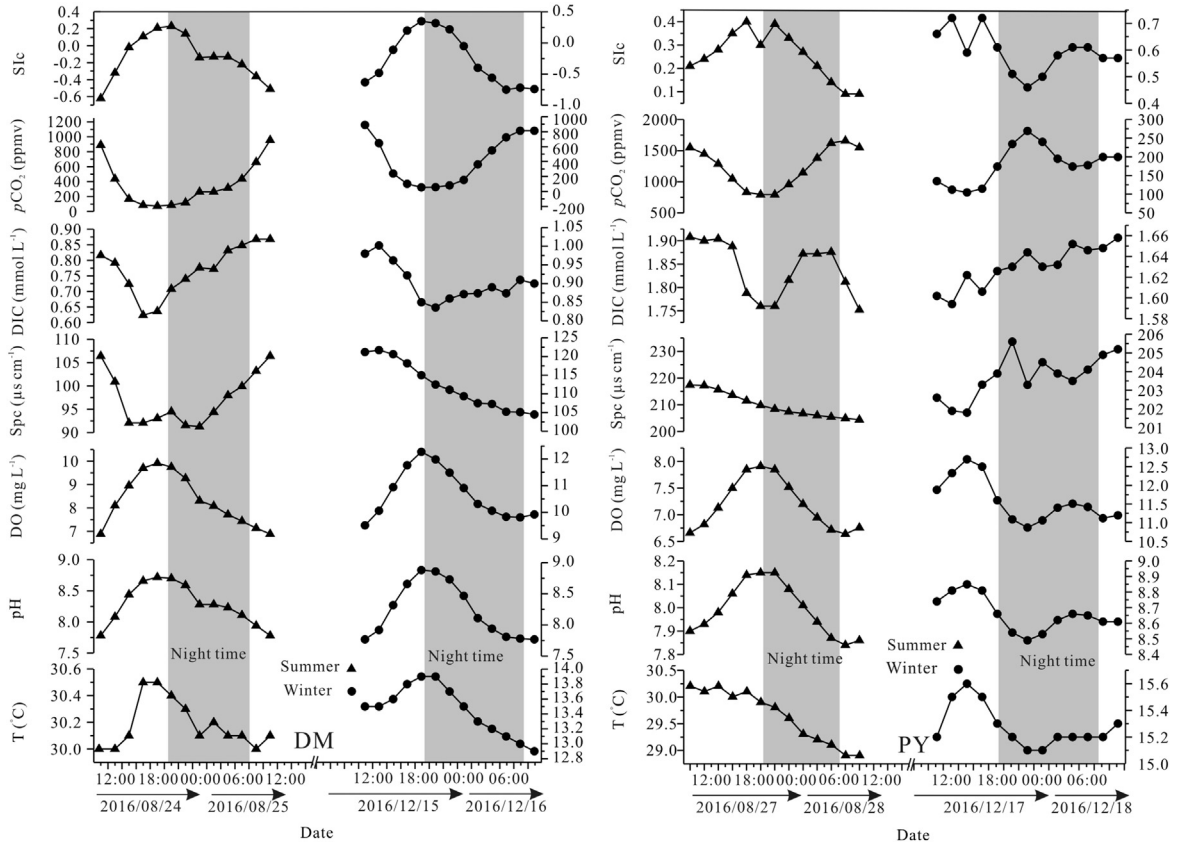

Fig. 2. The diurnal cycle of hydrochemical parameters at DM and PY transects.

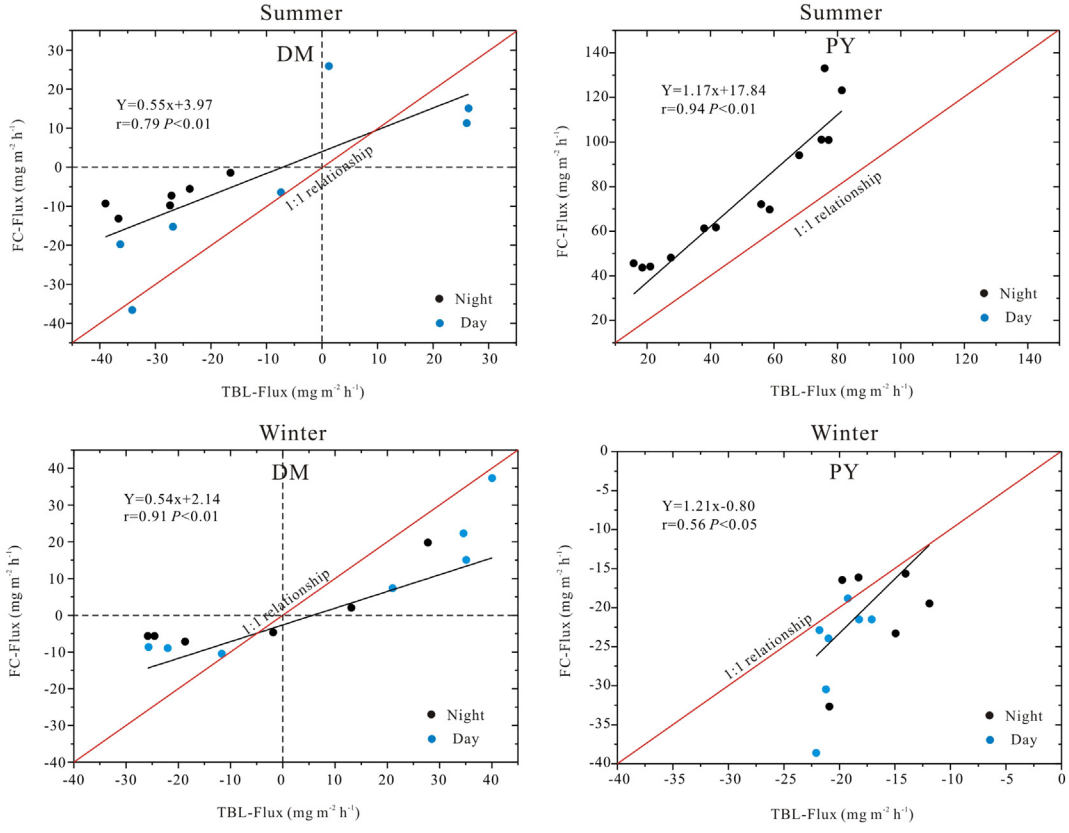

Fig. 3. Correlation between CO_2 fluxes across water-air interface calculated by TBL and FC methods.

consistency between the two methods. The FC method can be connected to real-time measurement systems, which allows simple and precise measurements (UNESCO/IHAGHG, 2010). Therefore, we use CO_2 fluxes estimated from FC method for further discussion in this paper. The values from TBL are presented only for comparison purposes.

3.3. Seasonal and diurnal variations of CO_2 degassing

Seasonal and diel variations occur in the magnitudes and directions of CO_2 fluxes at both transects during both sampling periods (Fig. 4A and B). At DM in summer, CO_2 fluxes ranged from −36.58 to 25.92 mg m^{-2} h^{-1} with the greatest flux occurring in the morning (10:00) and the smallest in late afternoon (16:00). In winter, fluxes varied from −10.59 to 37.38 mg m^{-2} h^{-1} with the greatest flux occurring in the morning (10:00) and the smallest in afternoon (14:00). At DM, the switch from evasion to adsorption occurred at noon (12:00 to 14:00) and from adsorption to evasion in early morning (4:00 to 6:00). At PY in the summer, CO_2 fluxes varied from 66.24 to 201.67 mg m^{-2} h^{-1} with the greatest flux occurring in the morning (10:00) and the smallest in the evening (18:00). In the winter, the fluxes ranged from −38.60 to −15.64 mg m^{-2} h^{-1} with the greatest CO_2 flux in the night (20:00) and the smallest at noon (12:00). In contrast with DM, the river at PY is a source of CO_2 to the atmosphere through the day and night in the summer, and a sink throughout the day and night in the winter. These results indicate that variations in processes cause karst rivers to alternate between atmospheric sources and sinks of CO_2 at both seasonal and diurnal time scales.

3.4. Factors controlling diel CO_2 flux

The pCO_2 variation in river waters depend on seasonal fluctuation of air temperature and precipitation (Yao et al., 2007) and storms can mute the diurnal signal of pCO_2 in stream waters (Peter et al., 2014). CO_2 fluxes also depend on ambient wind speed which alters the gas exchange coefficient (Therrien et al., 2005; Li et al., 2013). The study site received no rainfall over the monitoring periods. CO_2 flux had a weak but significant negative correlation with air temperature ($r = -0.56$, $P < 0.05$) at PY in the winter, and a weak but significant positive correlation with wind speed ($r = 0.65$, $P < 0.05$) at DM in the summer. These results indicate that some other factors are more important than local climatic conditions on the CO_2 fluxes across water-air interface in the GJR.

The magnitude and direction of CO_2 fluxes across the air-water interface depend on the air-water CO_2 concentration gradient (Hoffer-French and Herman, 1989) and diel variations in water temperature, which alters solubility of gases (Drysdale et al., 2003). CO_2 solubility decreases with increasing water temperature, which would increase CO_2 evasion from water that is supersaturated. However, water temperature and CO_2 fluxes showed a good negative correlation in both summer and winter at DM and in summer at PY (Fig. 5A and B) even though the water temperature showed little diel variation. Although a significant correlation exists, the mechanism causing the correlations could be related by other processes including calcite dissolution, photosynthesis, and respiration.

Both DO and CO_2 concentrations are controlled directly by diel variations in photosynthesis and respiration of subaquatic plants, algae, and microbes, and the change in pCO_2 also alters pH (Odum, 1956; Doctor et al., 2008). The DO concentration has strong negative correlations with pCO_2 and strong positive correlations with pH at both DM and PY regardless of the season (Fig. 5C, D, E and F). The correlation of DO with pCO_2 reflects photosynthesis and respiration in the sub-aquatic community. Correlation between pCO_2 and pH indicates that hydration of CO_2 is the primary acid in the system (Fig. 5G and H). Respiration-induced increases in pCO_2 should also affect CO_2 fluxes by increasing the gradient between the dissolved CO_2 and atmospheric pCO_2 (Carpenter et al., 2001; Pu et al., 2017). When the rate of photosynthesis exceeds the rate of respiration during the day, however, sufficient CO_2 is consumed in the river water to cause atmospheric CO_2 flux to the river. A positive correlation between pCO_2 and CO_2 fluxes at DM and PY in both summer and winter (Fig. 5I and J) suggest metabolic processes are a major controlling factor of CO_2 fluxes in the GJR. However, the nighttime flux out and daytime flux in doesn't happen at all seasons and places (Fig. 4A and B). For example, the nighttime flux out didn't happen at DM in both summer and winter (Fig. 4A), mainly because nighttime respiration increased the input of DIC and CO_2, decreased pH and increased calcite solubility, potentially driving calcite dissolution (de Montety et al., 2011; Kurz et al., 2013). This mechanism suggests that although the photosynthesis and respiration are important contributors to diurnal variations of CO_2 flux, these variations are also influenced by calcite precipitation/dissolution (e.g., de Montety et al., 2011).

This control of carbonate mineral influence on dissolved CO_2 concentrations (e.g., de Montety et al., 2011; Pu et al., 2017) is reflected in variation in the mineral saturation state of the water. As shown in Fig. 2, the SIc showed a diel pattern with high values at late afternoon and low values in morning or night at DM and PY in summer and winter, indicating the potential for calcite precipitation and increasing CO_2 evasion in the daytime. However, the river absorbed CO_2 in the daytime in summer and winter at DM and in winter at PY, and CO_2 evasion decrease during the day in summer at PY. These changes suggest that photosynthetic control of CO_2 fluxes masks the effects of calcite precipitation in the GJR.

The observed diurnal CO_2 fluxes in both summer and winter indicate the river switched from absorption and evasion of CO_2 at diurnal frequencies at DM but only at seasonal frequency at PY (Fig. 4A and B). Nonetheless, at DM, average pCO_2 and pH values changed little between seasons (Fig. 5G). However, at PY, average pCO_2 and pH were 6.9 and 1.1 times higher, respectively in summer than in winter (Fig. 5H). These

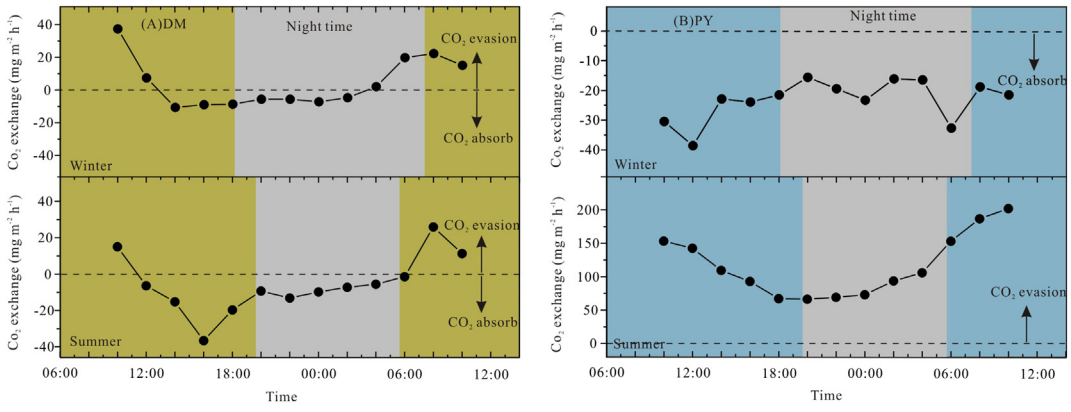

Fig. 4. Seasonal and diurnal variations of CO_2 fluxes across the water-air interface in the Guijiang River, southwest China.

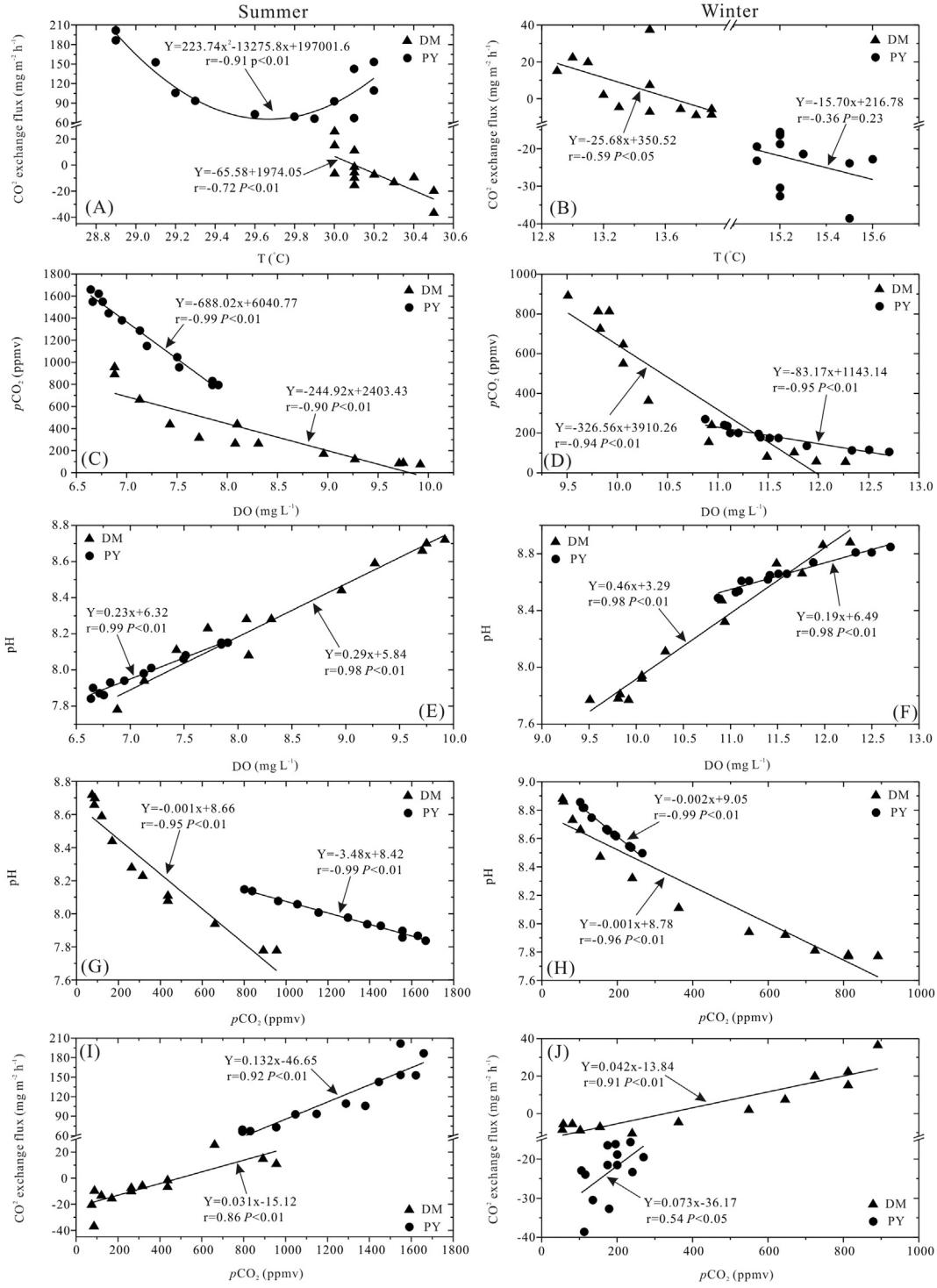

Fig. 5. Correlation between CO_2 flux and hydrochemical parameters.

observations contradict the expectation of a greater increase in pCO_2 in winter than summer caused by lower photosynthetic consumption of CO_2 due to less light. Turbid water could also affect photosynthesis and/or respiration, but the ΔTb and ΔpCO_2 showed no correlation ($r = 0.53$ $P = 0.06$), indicating that the seasonal variations of pCO_2 could be related by the carbon inputs. At PY, the minimum summer pCO_2 is 794.3 ppm, around 2 times higher than the atmospheric CO_2 value, while the maximum winter pCO_2 maximum value is 269.2 ppm, which is about 30% lower than atmospheric CO_2. These values indicate that, although diurnal variations of pCO_2 occur at PY, the seasonal changes control the overall pCO_2 and thus whether evasion and absorption occurs.

The major sources of carbon contributing to the total dissolved CO_2 in rivers include CO_2 derived from the decay of organic matter and the dissolution of carbonate minerals (e.g. Telmer and Veizer, 1999). Moreover, the multiple linear regression showed strong correlation between ΔFlux, ΔDIC, and ΔpH (ΔFlux = 3917.1–3.49ΔDIC + 361.0ΔpH, $R^2 = 0.84$, $P < 0.01$). pH is usually affected by the concentration of DIC in karst rivers, which decreases with the increasing DIC concentration (Pu, 2011). Therefore, the conversion between absorbing atmospheric

CO_2 in winter and degassing CO_2 in summer at PY was controlled by the seasonal changes of DIC input.

3.5. CO_2 fluxes relative to the world's inland water bodies

Since we used a 2 h sampling interval, the daily flux was calculated as (Li et al., 2014):

$$F_t = 2\sum F_{hi}/44 \quad (9)$$

where F_t is daily flux (mmol m^{-2} d^{-1}), F_h is the hourly flux (mmol m^{-2} h^{-1}), i is sampling time (10:00 to next day 08:00) and the sum covers all 12 samples. Whether it is daily flux or hourly flux, the positive fluxes represent CO_2 evasion while the negative fluxes represent CO_2 absorption.

The Guijiang River exhibited a CO_2 flux of 26 mmol m^{-2} d^{-1} in summer and −10 mmol m^{-2} d^{-1} in winter at PY, and exhibited a CO_2 flux of −11.3 mmol m^{-2} d^{-1} in winter and 0.3 mmol m^{-2} d^{-1} in summer at DM. The lowest value of CO_2 flux in the GJR occurred at DM in summer (−11.3 mmol m^{-2} d^{-1}), while the highest value was recorded at PY in summer (26 mmol m^{-2} d^{-1}) (Table 1). Most importantly, the river switches from an atmospheric carbon sink to an atmospheric carbon source on both seasonal and diurnal basis (Table 1). Although the net CO_2 flux is from the river to the atmosphere, the value is lower than most of the worlds' river systems. The low CO_2 degassing in the river is due to rapid kinetics of the carbonate minerals dissolution and photosynthetic uptake of river water DIC, as seen in other karst river systems (Khadka et al., 2014; Pu et al., 2017).

Further, there were major diurnal changes in CO_2 fluxes in GJR, in which the CO_2 fluxes vary by >170% in summer and >120% in winter at both DM and PY transects. The results indicate that global estimates of CO_2 exchange between rivers and atmosphere require information on diel variation in river water pCO_2 rather than single synoptic measurements. The accuracy of CO_2 fluxes could be greatly improved through the diel monitoring, particularly in the river with high primary productivity. Here, we introduce the contribution rate of hourly flux to the daily flux (Li et al., 2014):

$$a = \begin{cases} 2F_{hi}/F_t (F_t > 0) \\ 2F_{hi}/-F_t (F_t < 0) \end{cases} \quad (10)$$

where a represents the contribution rate of hourly flux to daily flux (%), with a positive for CO_2 evasion (F_t>0) while a is negative for CO_2 adsorption (F_t<0). The large diurnal variations in atmospheric fluxes, both into and out of the river (Fig. 6) demonstrate this need to evaluate the diurnal variations in river fluxes to estimate the seasonal as well as annual fluxes from the river.

Terrestrially derived carbon in inland water bodies may be buried in sediments, degassed to the atmosphere, or transported to the ocean (Battin et al., 2009; Aufdenkampe et al., 2011). Here we estimate the magnitude of CO_2 degassing rate and dissolved carbon fluxes output rate to the ocean. The CO_2 degassing rate to the atmosphere from the GJR is estimated to be 16 mmol m^{-2} d^{-1} based on the value at PY transect, which represent the upstream and middle reaches. Calculated flux output rate for DIC is 504 mmol m^{-2} d^{-1}. The CO_2 degassing from the GJR averages only 3.2% of the DIC flux out of the watershed. Our estimated proportion of CO_2 degassing to the DIC flux is almost the lowest of all reported tropical and temperate river systems (Telmer and Veizer, 1999; Polsenaere et al., 2012), and is similar to some carbonate rivers such as Changjiang River and Santa Fe River (Zai et al., 2007; Khadka et al., 2014). This lower CO_2 degassing rate reflects buffering by carbonate mineral dissolution of the CO_2 derived from soil and organic matter (Khadka et al., 2014). Overall, due to the strong photosynthetic uptake of river water DIC and rapid kinetics of the carbonate minerals dissolution, the GJR not only limits the CO_2 degassing, but also sequesters atmospheric carbon at diurnal and seasonal scales.

4. Conclusions

This study highlights the significant seasonal and diel variations in CO_2 fluxes across the water-air interfaces in a karst river. The variations are primarily driven by in-stream metabolic processes. The river switches from atmospheric carbon sink in winter to the atmospheric carbon source in summer. Further, the river alternatively consumes and degasses CO_2 during the day and night. These seasonal and diurnal variations in CO_2 fluxes indicate that significant uncertainty could exist in estimates of global riverine CO_2 emissions that disregard these diurnal and seasonal variations and consequently the impact of aquatic systems in global carbon cycle. We recommend seasonal and diurnal monitoring of CO_2 fluxes from the aquatic systems to minimize uncertainty in the estimates of CO_2 exchange between rivers and the

Table 1
Comparison of pCO_2 and CO_2 outgassing of the GJR with world rivers, lakes and reservoirs.

River	Sites	Climate	K (cm h^{-1})	Mean pCO_2(ppm_v)	CO_2 exchange (mmol m^{-2} d^{-1})	References
Guijiang(DM summer/winter)	China	Subtropic	5.8/3.9	366/422	−11.3/0.3	This study
Guijiang(PY summer/winter)	China	Subtropic	5.7/4.5	1236/179	26/−10	This study
Tigris	Turkey	Continental	11	1277	107.73	Varol and Li (2016)
Ottawa	Canada	Temperate	4	1200	80.8	Telmer and Veizer (1999)
Hudson	USA	Temperate	4	1125	15.9–37.0	Raymond et al. (1997)
Yukon		Boreal	20.4–31.7	>1500	171.2	Striegl et al. (2012)
St. Lawrence	Canada	Temperate	8–28	576	23.8–82.2	Yang et al. (1996)
Lower Mekong River		Tropic	26	1090	194.5	Li et al. (2013)
Eastmain, Quebec	Canada	Boreal	8.3	611	16.2	Teodoru et al. (2009)
Longchuan	China	Subtropic	8	2100	156.2	Li et al. (2012)
Amazon	Brazil	Tropic	10	4350	189.0	Richey et al. (2002)
Amazon	Brazil	Tropic	15	3320	345.2	Alin et al. (2011)
Xijiang	China	Subtropic	8–15	2600	189.0–356.2	Yao et al. (2007)
York River	USA	Warm		1070	22.7	Raymond et al. (2000)
Yangtze (Datong)	China	Subtropic	8	1297	38.4–147.9	Wang et al. (2007)
Mississippi		Temperate	16.3	1335	269.9	Dubois et al. (2010)
USA rivers				3120	202.7–915.1	Butman and Raymond (2011)
Hydroelectric reservoirs					32	Barros et al. (2011)
Nature lakes					28.8	Tranvik et al. (2009)
Artificial reservoirs waters					41	Barros et al. (2011)
Rivers				3230	93.2	Cole and Caraco (2001)
Rivers					146.8	Cole et al. (2007)
Rivers				2400	70.7	Lauerwald et al. (2015)

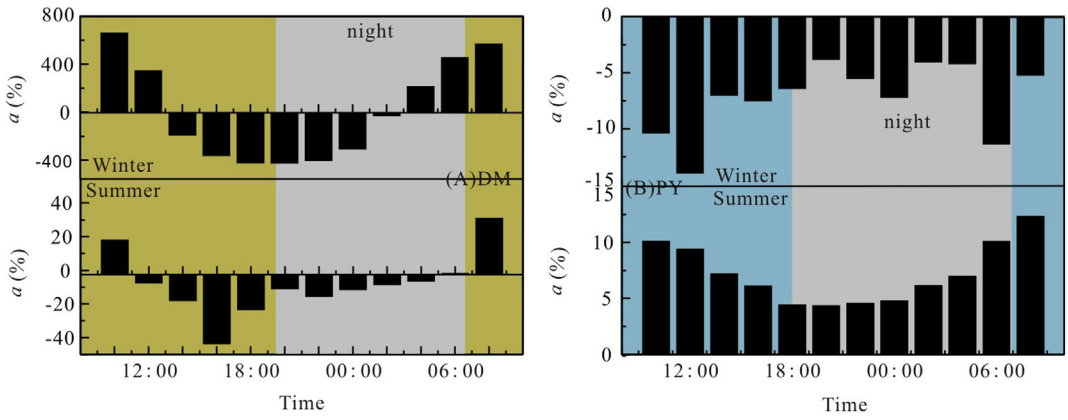

Fig. 6. Diel variations of the contribution percentage (a) of hourly flux to daily flux during the research.

atmosphere at global scales. This evaluation is particularly critical in karst river systems where the river waters are clear and enriched in dissolved carbon, which facilitates high primary productivity.

Conflict of interest

The authors declare no conflict of interest.

Acknowledgments

Financial support for this research was provided by National Natural Science Foundation of China (NO. 41572234, NO. 41202185), the Special Fund for Basic Scientific Research of Chinese Academy of Geological Sciences (NO. YYWF201636), the Key Research & Development Fund of Ministry of Science and Technology of China (NO. 2016YFC0502501), the Guangxi Natural Science Foundation (2016GXNSFCA380002), the Geological Survey Project of CGS (DD20160305-03), and the US NSF (EAR-0938369 and EAR-0853956 to JBM).

References

Alin, S.R., de Fátima, F.L., Rasera, M., Salimon, C.I., Richey, J.E., Holtgrieve, G.W., Krusche, A.V., Snidvongs, A., 2011. Physical controls on carbon dioxide transfer velocity and flux in low-gradient river systems and implications for regional carbon budgets. J. Geophys. Res. Biogeosci. 116 (G1).

Aufdenkampe, A.K., Mayorga, E., Raymond, P.A., Melack, J.M., Doney, S.C., Alin, S.R., Aalto, R.E., Yoo, K., 2011. Riverine coupling of biogeochemical cycles between land, oceans, and atmosphere. Front. Ecol. Environ. 9, 53–60.

Barros, N., Cole, J.J., Tranvik, L.J., Prairie, Y.T., Bastviken, D., Huszar, V.L.M., del Giorgio, P., Roland, F., 2011. Carbon emission from hydroelectric reservoirs linked to reservoir age and latitude. Nat. Geosci. 4, 593–596.

Battin, T.J., Luyssaert, S., Kaplan, L.A., Aufdenkampe, A.K., Richter, A., Tranvik, L.J., 2009. The boundless carbon cycle. Nat. Geosci. 2, 598–600.

Bauer, J.E., Cai, W.J., Raymond, P.A., Bianchi, T.S., Hopkinson, C.S., Regnier, P.A.G., 2013. The changing carbon cycle of the coastal ocean. Nature 504, 61–70.

Borges, A.V., Darchambeau, F., Teodoru, C.R., Marwick, T.R., Tamooh, F., Geeraert, N., Omengo, F.O., Guérin, F., Lambert, T., Morana, C., Okuku, E., Bouillon, S., 2015. Globally significant greenhouse-gas emissions from African inland waters. Nat. Geosci. 2015 (8), 637–642.

Butman, D., Raymond, P.A., 2011. Significant efflux of carbon dioxide from streams and rivers in the United States. Nat. Geosci. 4, 839–842.

Carpenter, S.R., Cole, J.J., Hodgson, J.R., Kitchell, J.F., Pace, M.L., Bade, D., Cottingham, K.L., Essington, T.E., Houser, J.N., Schindler, D.E., 2001. Trophic cascades, nutrients, and lake productivity: whole-lake experiments. Ecol. Monogr. 71, 163–186.

Cole, J.J., Caraco, N.F., 2001. Carbon in catchments: connecting terrestrial carbon losses with aquatic metabolism. Mar. Freshw. Res. 52, 101–110.

Cole, J.J., Prairie, Y.T., Caraco, N.F., McDowell, W.H., Tranvik, L.J., Striegl, R.G., Duarte, C.M., Kortelainen, P., Downing, J.A., Middelburg, J.J., Melack, J., 2007. Plumbing the global carbon cycle: integrating inland waters into the terrestrial carbon budget. Ecosystems 10, 172–185.

de Montety, V., Martin, J.B., Cohen, M.J., Foster, C., Kurz, M.J., 2011. Influence of diel biogeochemical cycles on carbonate equilibrium in a karst river. Chem. Geol. 283, 31–43.

Degens, E.T., Kempe, S., Richey, J.E., 1991. Summary: biogeochemistry of major world rivers. In: Degens, E.T., Kempe, S., Richey, J.E. (Eds.), Scientific Committee on Problems of the Environment (SCOPE)/United Nations Environment Programme (UNEP)—Biogeochemistry of Major World Rivers. Vol. 42. Chichester, U.K. John Wiley & Sons, pp. 323–347.

Doctor, D.H., Kendall, C., Sebestyen, S.D., Shanley, J.B., Ohte, N., Boyer, E., 2008. Carbon isotope fractionation of dissolved inorganic carbon (DIC) due to outgassing of carbon dioxide from a headwater stream. Hydrol. Process. 22:2410–2423. http://dx.doi.org/10.1002/hyp.

Drysdale, R., Lucas, S., Carthew, K., 2003. The influence of diurnal temperatures on the hydrochemistry of a tufa-depositing stream. Hydrol. Process. 17:3421–3441. http://dx.doi.org/10.1002/hyp.1301.

Dubois, K.D., Lee, D., Veizer, J., 2010. Isotopic constraints on alkalinity, dissolved organic carbon, and atmospheric carbon dioxidefluxes in the Mississippi River. J. Geophys. Res. 115, G02018.

Duchemin, E., Lucotte, M., Canuel, R., 1999. Comparison of static chamber and thin boundary layer equation methods for measuring greenhouse gas emissions from large water bodies. Environ. Sci. Technol. 1999 (33), 350–357.

Hoffer-French, K.J., Herman, J.S., 1989. Evaluation of hydrological and biological influences on CO_2 fluxes from a karst stream. J. Hydrol. 108, 189–212.

Jones, J.B., Stanley, E.H., Mulholland, P.J., 2003. Long-term decline in carbon dioxide supersaturation in rivers across the contiguous United States. Geophys. Res. Lett. 30, 1495.

Khadka, M.B., Martin, J.B., Jin, J., 2014. Transport of dissolved carbon and CO_2 degassing from a river system in a mixed silicate and carbonate catchment. J. Hydrol. 513, 391–402.

Kurz, M.J., de Montety, V., Martin, J.B., Cohen, M.J., Foster, C.R., 2013. Controls on diel metal cycles in a biologically productive carbonate-dominated river. Chem. Geol. 358, 61–74.

Lambert, M., Fréchette, J.L., 2005. Analytical Techniques for Measuring Fluxes of CO_2 and CH_4 from Hydroelectric Reservoirs and Natural Water Bodies. Greenhouse Gas Emissions—Fluxes and Processes. Springer, Berlin Heidelberg, pp. 37–60.

Lauerwald, R., Laruelle, G.G., Hartmann, J., Ciais, P., Regnier, P.A.G., 2015. Spatial patterns in CO_2 evasion from the global river network. Glob. Biogeochem. Cycles 29.

Li, S.Y., Lu, X.X., He, M., Zhou, Y., Li, L., Ziegler, A.D., 2012. Daily CO_2 partial pressure and CO_2 outgassing in the upper Yangtze River basin: a case study of the Longchuan River, China. J. Hydrol. 466–467.

Li, S.Y., Lu, X.X., Bush, R.T., 2013. CO_2 partial pressure and CO_2 emission in the lower Mekong River. J. Hydrol. 504, 40–56.

Li, Zhe, Yao, Xiao, He, Ping, Wang, Qin, Guo, Jinsong, Chen, Yongbo, 2014. Diel variations of air-water CO_2 and CH_4 diffusive fluxes in the Pengxi River, Three Gorges Reservoir. J. Lake Sci. 26, 576–584 (In chinese).

Liu, Z.H., Li, Q., Sun, H.L., Liao, C.J., Li, H.J., Wang, J.L., Wu, K.Y., 2006. Diurnal variations of hydrochemistry in a travertine-depositing stream at Baishuitai, Yunnan, SW China. Aquat. Geochem. 12, 103–121.

Liu, Z.H., Liu, X.L., Liao, C.J., 2008. Daytime deposition and nighttime dissolution of calcium carbonate controlled by submerged plants in a karst spring-fed pool: insights from high time-resolution monitoring of physico-chemistry of water. Environ. Geol. 55, 1159–1168.

Liu, W., Pu, J.B., Zhang, C., 2014. A portable greenhouse gas collection equipment in water and land dual-use. China Patent. ZL 201420363633. 4.(In Chinese).

Martin, J.B., 2017. Carbonate minerals in the global carbon cycle. Chem. Geol. 449, 58–72.

Nimick, D.A., Gammons, C.H., Parker, S.R., 2011. Diel biogeochemical processes and their effect on the aqueous chemistry of streams: a review. Chem. Geol. 283, 3–17.

Odum, H.T., 1956. Primary production inflowing waters. Limnol. Oceanogr. 1, 102–117.

Peter, H., Singer, G.A., Preiler, C., Chifflard, P., Steniczka, G., Battin, T.J., 2014. Scales and drivers of temporal pCO_2 dynamics in an alpine stream. J. Geophys. Res. 119, 1078–1091.

Polsenaere, P., Savoye, N., Etcheber, H., Canton, M., Poirier, D., Bouillon, S., Abril, G., 2012. Export and degassing of terrestrial carbon through watercourses draining a temperate podzolized catchment. Aquat. Sci. 75, 299–319.

Pu, J., 2011. Research on the Controlling Factors of Formation and Distribution of Subterranean Karst Streams and Its Hydrogeochemistry Regionality, Chongqing. Southwest University, China.

Pu, J., Li, J., Khadka, M.B., Martin, J.B., Zhang, T., Yu, S., Yuan, D.X., 2017. In-stream metabolism and atmospheric carbon sequestration in a groundwater-fed karst stream. Sci. Total Environ. 579, 1343–1355.

Raymond, P.A., Caraco, N.F., Cole, J.J., 1997. Carbon dioxide concentration and atmospheric flux in the Hudson River. Estuaries 20, 381–390.

Raymond, P.A., Bauer, J.E., Cole, J.J., 2000. Atmospheric CO_2 evasion, dissolved inorganic carbon production, and net heterotrophy in the York River estuary. Limnol. Oceanogr. 45, 1707–1717.

Raymond, P.A., Zappa, C.J., Butman, D., Bott, T.L., Potter, J., Mulholland, P., Laursen, A.E., McDowell, W.H., Newbold, D., 2012. Scaling the gas transfer velocity and hydraulic geometry in streams and small rivers [J]. Limnol. Oceanogr. Fluids Environ. 2, 41–53.

Raymond, P.A., Hartmann, J., Lauerwald, R., Sobek, S., McDonald, C., Hoover, M., Butman, D., Striegl, R., Mayorga, E., Humborg, C., Kortelainen, P., Dürr, H., Meybeck, M., Ciais, P., Guth, P., 2013. Global carbon dioxide emissions from inland waters. Nature 503, 355–359.

Regnier, P., Friedlingstein, P., Ciais, P., Mackenzie, F.T., Gruber, N., Janssens, I.A., Laruelle, G.G., Lauerwald, R., Luyssaert, S., Andersson, A.J., Arndt, S., Arnosti, C., Borges, A.V., Dale, A.W., Gallego-Sala, A., Goddéris, Y., Goossens, N., Hartmann, J., Heinze, C., Llyina, T., Joos, F., LaRowe, D.E., Leifeld, J., Meysman, F.J.R., Munhoven, G., Raymond, P.A., Spahni, R., Suntharalingam, P., Thullner, M., 2013. Anthropogenic perturbation of the carbon fluxes from land to ocean. Nat. Geosci. 6, 597–607.

Rice, E.W., Baird, R.B., Eaton, A.D., Clesceri, L.S., 2012. Standard Methods for the Examination of Water and Wastewater. 22nd ed. American Public Health Association, the American Water Works Association and the Water Environment Federation, Washington D.C.

Richey, J.E., Melack, J.M., Aufdenkampe, A.K., Ballester, V.M., Hess, L.L., 2002. Outgassing from Amazonian rivers and wetlands as a large tropical source of atmospheric CO_2. Nature 416, 617–620.

Sarmiento, J.L., Sundquist, E.T., 1992. Revised budget for the oceanic uptake of anthropogenic carbon dioxide. Nature 356, 589–593.

Striegl, R.G., Dornblaser, M.M., McDonald, C.P., Rover, J.R., Stets, E.G., 2012. Carbon dioxide and methane emissions from the Yukon River system. Glob. Biogeochem. Cycles 26, GB0E05.

Sun, H.G., Han, J.T., Zhang, S.R., Lu, X.X., 2015. Carbon isotopic evidence for transformation of DIC to POC in the lower Xijiang River, SE China. Quat. Int. 380, 288–296.

Telmer, K., Veizer, J., 1999. Carbon fluxes, pCO_2 and substrate weathering in a large northern river basin, Canada: carbon isotope perspectives. Chem. Geol. 159, 61–86.

Teodoru, C.R., del Giorgio, P.A., Prairie, Y.T., Camire, M., 2009. Patterns in pCO_2 in boreal streams and rivers of northern Quebec, Canada. Glob. Biogeochem. Cycles 23, GB2012.

Therrien, J., Tremblay, A., Jacques, R.B., 2005. CO_2 emissions from semi-arid reservoirs and natural aquatic ecosystems. Greenhouse Gas Emissions—Fluxes and Processes. Springer Berlin Heidelberg, pp. 233–250.

Tranvik, L.J., Downing, J.A., Cotner, J.B., Loiselle, S.A., Striegl, R.G., Ballatore, T.J., Dillon, P., Finlay, K., Fortino, K., Knoll, L.B., Kortelainen, P.L., Kutser, T., Larsen, S., Laurion, I., Leech, D.M., McCallister, S.L., McKnight, D.M., Melack, J.M., Overholt, E., Porter, J.A., Prairie, Y., Renwick, W.H., Roland, F., Sherman, B.S., Schindler, D.W., Sobek, S., Tremblay, A., Vanni, M.J., Verschoor, A.M., Wachenfeldt, E.V., Weyhenmeyer, G.A., 2009. Lakes and reservoirs as regulators of carbon cycling and climate [J]. Limnol. Oceanogr. 54, 2298–2314.

UNESCO/IHA GHG, 2010. Greenhouse gas emissions related to freshwater reservoirs. World Bank Report, pp. 64–127.

Varol, M., Li, S., 2016. Biotic and abiotic controls on CO_2 partial pressure and CO_2 emission in the Tigris River, Turkey. Chem. Geol. 449, 182–193.

Wang, F.S., Wang, Y.C., Zhang, J., Xu, H., Wei, X.G., 2007. Human impact on the historical change of CO_2 degassing flux in river Changjiang. Geochem. T. 8, 1–10.

Wigley, T.M.L., 1977. WATSPEC: a computer program for determining the equilibrium speciation of aqueous solutions. Geo-Abstracts for the British Geomorphological Research Group, pp. 1–49.

Yang, C., Telmer, K., Veizer, J., 1996. Chemical dynamics of the "St. Lawrence" riverine system: δD_{H_2O}, $\delta^{18}O_{H_2O}$, $\delta^{13}C_{DIC}$, $\delta^{34}S_{sulfate}$, and dissolved $^{87}Sr/^{86}Sr$. Geochim. Cosmochim. Ac. 60, 851–866.

Yao, G.R., Gao, Q.Z., Wang, Z.G., Huang, X.K., He, T., Zhang, Y.L., Jiao, S.L., Ding, J., 2007. Dynamics of CO_2 partial pressure and CO_2 outgassing in the lower reaches of the Xijiang River, a subtropical monsoon river in China. Sci. Total Environ. 376, 255–266.

Zai, W., Dai, M., Guo, X., 2007. Carbonate system and CO2degassing fluxes in the inner estuary of Changjiang (Yangtze) river, China. Mar. Chem. 107, 342–356.

Zhao, Y., Sherman, B., Ford, P., Demarty, M., DelSontro, T., Harby, A., Tremblay, A., Øverjordet, I.B., Zhao, X.Y., Hansen, B.H., Wu, B.F., 2015. A comparison of methods for the measurement of CO_2 and CH_4 emissions from surface water reservoirs: results from an international workshop held at Three Gorges Dam, June 2012. Limnol. Oceanogr. Methods 13, 15–29.